

Persistent spectral-hole-burning spectroscopy of CuCl quantum cubes

著者	Sakakura Naru, Masumoto Yasuaki
journal or publication title	Physical review B
volume	56
number	7
page range	4051-4055
year	1997-08
権利	(C)1997 The American Physical Society
URL	http://hdl.handle.net/2241/98264

doi: 10.1103/PhysRevB.56.4051

Persistent spectral-hole-burning spectroscopy of CuCl quantum cubes

Naru Sakakura* and Yasuaki Masumoto†

Institute of Physics and Center for TARA (Tsukuba Advanced Research Alliance), University of Tsukuba, Tsukuba, Ibaraki 305, Japan

(Received 26 March 1997)

A persistent spectral-hole-burning (PSHB) phenomenon was successfully applied to the precise site-selective spectroscopy of CuCl quantum dots embedded in NaCl crystals. In the PSHB spectra of CuCl quantum dots, a resonantly burned hole and lower-energy satellite holes were observed. These satellite holes are supposed to originate from hole burning of the ground states, which results from site-selective excitation of the corresponding excited states of excitons confined in CuCl quantum dots. Energy relation between the resonantly burned hole and each satellite hole is well explained by the simple concept of a particle in a quantum cube with an infinitely high potential barrier. However, actual quantum dots are considered to be a little deviated from cubes, resulting in the violation of the optical selection rule in quantum cubes. A cubic-shaped quantum-dot model is almost consistent with oscillatory fine structures observed in the Z_3 exciton absorption band. Its spectral decomposition into the ground state and the first excited state of excitons was made, and showed that the first excited state is in majority at the higher-energy region of the Z_3 exciton absorption band. This result was supported by the photoluminescence spectrum of the Z_3 exciton. [S0163-1829(97)07632-7]

In nanometer-size semiconductor crystallites, or zero-dimensional quantum dots, electronic and optical properties are dramatically different from those in three-dimensional bulk semiconductors. As a result, they have been attracting much interest not only from the viewpoint of fundamental physics but also from the expectation for their potential applications to various electronic and optical devices such as a quantum-dot laser. For application, it is very important to understand and control the physical properties of ordered quantum dots. Orders of quantum dots are classified as those in size, alignment, orientation, and shape. Ordering quantum dots in size is of major importance, because the size distribution of quantum dots is the primary source of inhomogeneous broadening that can completely cancel out the advantages of zero-dimensional density of states. Narrow distribution in dot size has been performed for self-organized $\text{In}_x\text{Ga}_{1-x}\text{As}/\text{GaAs}$ quantum dots grown by molecular-beam epitaxy¹ and by metalorganic chemical vapor deposition (MOCVD),² and for colloidal CdSe quantum dots.³ As for the order in alignment, an aligned array of $\text{GaAs}/\text{Al}_x\text{Ga}_{1-x}\text{As}$ quantum dots was fabricated by using electron-beam lithography and plasma etching, although the size of each quantum dot is as large as 57 nm in diameter.⁴ A self-alignment of the smaller self-organized $\text{In}_x\text{Ga}_{1-x}\text{As}/\text{GaAs}$ quantum dots grown by MOCVD was recently achieved.^{5,6} In the case of orientational order, the crystal axis of CuCl quantum dots and that of the NaCl matrix were found to be parallel to each other.⁷ Order in dot shape, however, has been little studied. One of the purposes in this paper is to investigate the shape of CuCl quantum dots embedded in NaCl crystals by means of persistent spectral hole burning (PSHB) spectroscopy.

Recently, PSHB phenomenon in semiconductor quantum dots such as CuCl, CuBr, CuI, CdSe, CdTe, and CdS quantum dots embedded in glass, crystals, or polymers has been observed.^{8–13} Ever since, the PSHB is considered to be applicable to the precise site-selective spectroscopy of quantum dots. When the spectrally narrow light excites the inhomoge-

neously broadened absorption band, a spectral hole is formed at the position of the excitation photon energy in the absorption band, and the spectral hole is preserved for a long time at low temperature. As a result of the PSHB, the electronic and excitonic quantum states, including the excited states, may be burned. This allows us to investigate the energies of quantum dots systematically. Because the energies of quantum dots depend on their shape, the precise study of the energies by means of PSHB spectroscopy is useful for the investigation of the shape of CuCl quantum dots. Another purpose of this paper is to investigate the correlation between the ground- and the excited-state excitons confined in CuCl quantum dots in NaCl crystals by means of PSHB spectroscopy.

Samples, CuCl quantum dots in NaCl, were made from the melted mixture of NaCl and CuCl, and grown by the transverse Bridgman method. The as-grown crystals were cleaved into several pieces and were annealed in Ar atmosphere for the control of the size distribution of CuCl quantum dots. The samples were directly immersed in superfluid helium at 2 K or mounted on a sample rod of a temperature variable cryostat. A spectrally narrow dye laser pumped by a Q -switched Nd^{3+} : YAG (yttrium aluminum garnet) laser was used as a pump source. The spectral width of the dye laser was 0.014 meV and the pulse duration was approximately 5 ns. The repetition rate of the laser system was 30 Hz. A halogen lamp was used as a probe source. The transmittance of the probe beam was detected by using a liquid-nitrogen-cooled charge-coupled-device optical multichannel analyzer in conjunction with a 75 cm monochromator. The spectral resolution of the experiment was 0.04 nm (0.35 meV). For the luminescence measurements, the third-harmonic light of the Nd^{3+} : YAG laser (355 nm, 3.49 eV) was used as a band-to-band excitation source.

It is known that photoexcited exciton in CuCl quantum dots is confined in the limited space and that its center-of-mass translational motion is quantized due to a small exciton Bohr radius of 0.68 nm.^{14,15} Figure 1 shows absorption spec-

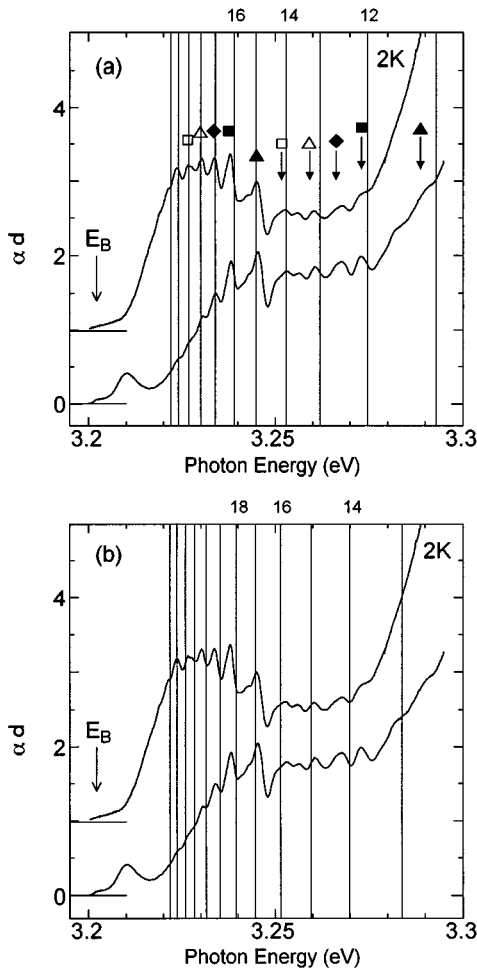


FIG. 1. Z_3 exciton absorption spectra of CuCl quantum dots in NaCl crystals at 2 K. Vertical solid lines in (a) and (b) indicate the calculated energies of the Z_3 exciton under the assumption of quantum cubes and spheres, respectively. E_B is the bulk Z_3 exciton energy.

tra of CuCl quantum dots in NaCl crystals at 2 K. Oscillatory fine structures are observed between 3.22 and 3.28 eV in the inhomogeneously broadened Z_3 exciton absorption band.¹⁶ Origin of the inhomogeneous broadening has been explained partly by the size distribution of the quantum dots. Itoh *et al.* suggested that each oscillatory fine structure was explained by the size-quantized lowest energy of the Z_3 exciton confined in a quantum cube whose side changes stepwise in a unit of $a/2$, where a is a lattice constant of CuCl crystal.¹⁷ If an infinitely tall potential barrier is assumed in a CuCl quantum cube with the side length of L , quantized exciton energy levels are easily derived from the simple concept of a particle in a quantum cube and are described by

$$E_{n_x, n_y, n_z} = E_B + \frac{\hbar^2 \pi^2}{2M(L - a_B)^2} (n_x^2 + n_y^2 + n_z^2), \quad (1)$$

where E_B is the bulk Z_3 exciton energy ($E_B = 3.2022$ eV), M is the translational mass of exciton ($M = 2.3m_0$), a_B is its Bohr radius ($a_B = 0.68$ nm), quantum numbers n_x , n_y , and n_z , take values 1, 2, 3, ..., and $(L - a_B)$ is used for the dead layer correction. Vertical solid lines in Fig. 1(a) indicate the

expected energy of the ground state $E_{1,1,1}$ in cubes with the side length of each cube shown at the top in a unit of half the lattice constant a ($a = 0.54$ nm).

On the other hand, if quantum dots are assumed to be a sphere with radius R and its diameter changes stepwise in a unit of $a/2$, quantized energy levels are calculated by

$$E_{n,l} = E_B + \frac{\hbar^2 \pi^2}{2M(R - a_B/2)^2} \xi_{n,l}^2, \quad (2)$$

where $\pi \xi_{n,l}$ is the n th root of the spherical Bessel function of the l th order and the principal quantum number n and the angular momentum quantum number l take values $n = 1, 2, 3, \dots$ and $l = 0, 1, 2, \dots$, respectively. $\xi_{n,l}$ takes values $\xi_{1,0} = 1$, $\xi_{1,1} = 1.4303$, $\xi_{1,2} = 1.8346$, $\xi_{2,2} = 2$, and so on. For the dead layer correction, $(R - a_B/2)$ is used. Vertical solid lines in Fig. 1(b) represent the calculated energy of the ground state $E_{1,0}$ with the diametric length of each sphere shown at the top in a unit of half the lattice constant a . The oscillatory fine structure below 3.25 eV is better fitted by $E_{1,1,1}$ rather than by $E_{1,0}$ and suggests that the shape of CuCl quantum dots is cubic rather than spherical. However, above 3.25 eV, the peak energies of the oscillatory fine structures do not coincide with the calculated energies for both quantum cubes and spheres. It also should be commented that the experimental peaks can be explained neither by the quantum sphere model nor the quantum cube model without the dead layer correction.

In order to explain peaks above 3.25 eV, the first excited state of excitons confined in CuCl quantum cubes was taken into account. They are well fitted by the first excited-state energy $E_{2,1,1}$ calculated on the basis of the energy relation $E_{2,1,1} - E_B = 2(E_{1,1,1} - E_B)$ obtained from Eq. (1), as shown by downward arrows with ▲, ■, ◆, △, and □ in Fig. 1(a). Here, the first excited-state energy $E_{2,1,1}$ denoted by downward arrows with ▲, ■, ◆, △, and □ above 3.25 eV is calculated by the peak position of the ground-state energy $E_{1,1,1}$ denoted by ▲, ■, ◆, △, and □ below 3.25 eV, respectively. In this way, the observed peaks above 3.25 eV are energetically explained by the first excited states of excitons in CuCl quantum cubes. The optical selection rule, however, tells us that the first excited exciton state $E_{2,1,1}$ confined in a quantum cube does not contribute to the optical transitions because of the parity.^{18,19} The exciton wave function for the center-of-mass motion is simply given by sine functions with quantum number n , which has even parity for the states of odd n and odd parity for those of even n . Integration of the wave functions over the cube gives the matrix element of the electric dipole transition between the ground and the n th state, and the matrix element is equal to zero for even quantum number n , according to the long-wavelength approximation. The reason why the optical selection rule is broken is discussed later.

Absorption and absorption change spectra of CuCl quantum dots at 2 K are shown in Figs. 2(a) and 2(b), respectively. The absorption change spectrum $-\Delta\alpha d$ is defined by the absorption spectrum of the sample exposed to the narrow-band dye laser minus that of the virgin sample. The sample was exposed to 72 000 shots of dye laser pulses with the photon energy of 3.2378 eV and excitation density of 46 nJ/cm². In addition to the spectral hole resonantly burned

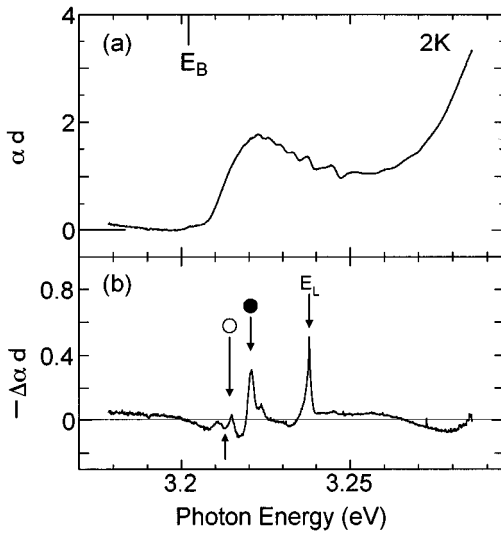


FIG. 2. Absorption (a) and absorption change (b) spectra in CuCl quantum dots in NaCl at 2 K. Excitation photon energy denoted by E_L is 3.2378 eV. Structures marked by a solid circle and an open circle show the spectral holes observed at $E = E_B + (E_L - E_B)/n$, where n takes values 2 and 3, respectively. An upward arrow indicates the position at $E = E_B + (E_L - E_B)/3.35$.

at the excitation photon energy denoted by E_L , lower-energy satellite holes were also burned at energy position E , where E satisfies $E_L - E_B = n(E - E_B)$ with $n=2$ or 3. Solid and open circles in Fig. 2(b) show the satellite holes for cases $n=2$ and 3, respectively. The appearance of these satellite holes can be explained as follows: if quantized exciton energy levels are described by Eq. (1), the ground state $E_{1,1,1}$ and the first and the second excited states $E_{2,1,1}, E_{2,2,1}$ satisfy the relations $E_{2,1,1} - E_B = 2(E_{1,1,1} - E_B)$ and $E_{2,2,1} - E_B = 3(E_{1,1,1} - E_B)$, respectively. Site-selective excitation of the excited states results in hole burning of the corresponding ground state, which is observed as the lower-energy satellite holes in Fig. 2(b). Although the state $E_{2,2,1}$ was excited, hole burning of the state $E_{2,1,1}$ relaxed from the $E_{2,2,1}$ state was not observed experimentally and only the ground state $E_{1,1,1}$ was burned. This suggests that the relaxation from the excited state to the ground state is considered to be much faster than the persistent spectral hole burning process and the recombination of the ground-state excitons. If quantum dots are assumed to be spheres, and if the second excited state is burned, the resultant satellite holes should appear in the energy positions marked by an upward arrow in Fig. 2(b). Absence of burned hole at the upward arrow indicates that the shape of CuCl quantum dots in NaCl matrix is cubic rather than spherical and that quantized exciton energy levels are described by Eq. (1). However, it should be noted that the optical transitions to both the first and second excited states are forbidden and the appearance of satellite holes cannot be explained by the excited states of excitons confined in ideal CuCl quantum cubes.

Figure 3 shows satellite hole positions E as a function of the excitation photon energy E_L . Several samples were used for this measurement. Solid circles and open circles correspond to the burned satellite holes of the ground states $E_{1,1,1}$, which result from the laser resonant excitation of the first excited states $E_{2,1,1}$ and the second excited states

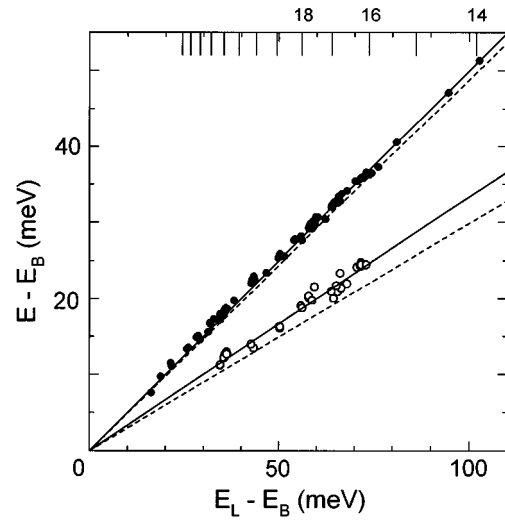


FIG. 3. Spectral hole positions E as a function of the excited photon energy E_L for CuCl quantum dots in NaCl. Solid circles and open circles are explained in the text. Calculated excited states for quantum cubes and for quantum spheres are shown by a solid line and a dashed line, respectively. The size of cubes in which the first excited states of excitons are confined is shown by the top long scale in a unit of half the lattice constant.

$E_{2,2,1}$, respectively. The corresponding calculated satellite hole positions based on Eqs. (1) and (2) are shown by solid and dashed lines, respectively. Although open circles are slightly scattered, agreement of experimental data and calculated results based on Eq. (1) is good. We should notice that satellite holes marked by solid circles move almost continuously, although the first excited exciton states $E_{2,1,1}$ confined in ideal quantum cubes shift discretely as shown by the long scale at the top horizontal axis. This feature can be understood under the following assumptions: Energies of the first excited-state excitons confined in quantum dots, whose shapes are a little deviated from an ideal cube, are expressed by $E_{2,1,1} - E_B = 2(E_{1,1,1} - E_B)$ but the deviation is not so large to be a sphere. This possibility should be examined from the point of view of the selection rule. As mentioned before, if the shape of quantum dots is an ideal cube, the first excited state $E_{2,1,1}$ and the second excited state $E_{2,2,1}$ do not contribute to the optical transitions and solid and open circles in Fig. 3 should not appear. Our experimental results, that the excited states $E_{2,1,1}$ and $E_{2,2,1}$ are optically found, suggest that all of the dots are not ideal quantum cubes and that deviation from the cubic shape violates the selection rule.

One may consider strain between CuCl quantum dots and NaCl matrix or built-in electric field caused by trapped carriers is a possible origin of the violation of the selection rule. Hydrostatic pressure from the NaCl surrounding matrix may be applied to CuCl quantum dots, but the energy shift caused by the pressure was shown to be too small to explain the size-dependent energy shift of the exciton transition.¹⁵ Moreover, isotropic hydrostatic pressure cannot be considered to give the violation of the selection rule. The selection rule in CuCl quantum cubes comes from the parity of the envelope function of exciton, which describes the exciton translational motion. It is different from the selection rule for dots in the strong confinement regime, where the selection rule comes

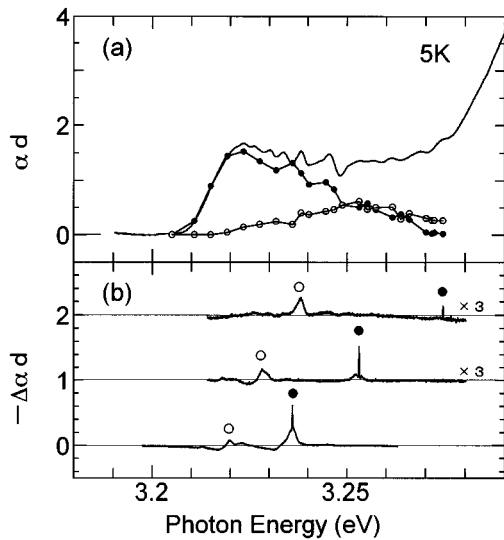


FIG. 4. An absorption spectrum (a) and absorption change spectra (b) of CuCl quantum dots in NaCl at 5 K. Solid and open circles in (a) represent the spectral profiles of the ground states and the first excited states in CuCl quantum dots, respectively.

from the parity of the envelope functions of the electrons and holes and is violated by the electric field.²⁰ Built-in electric field in the quantum dots can cause electron-hole separation in exciton and therefore change the internal motion of exciton, but cannot change the envelope function of exciton. This consideration excludes the electric field as an origin to violate the selection rule.

Figure 4 shows absorption (a) and absorption change (b) spectra with three excitation photon energies marked by solid circles. Excitation energies are 3.2745, 3.2531, and 3.2360 eV from top to bottom. Accumulated excitation energy density is 6 mJ/cm². It is apparent from Fig. 4(b) that the ratio of the satellite hole area (○) to the resonantly burned hole area (●) increases with the increase of the burning photon energy. This indicates that the contribution of the first excited states to the absorption band increases with the increase of the photon energy compared with that of the ground states. The resonantly burned hole is supposed to come from the ground states at the burning photon energy and not to contain the excited states as a result of the fast relaxation from the excited state to the ground state. Therefore, the ratio of the resonantly burned hole area (●) to the satellite hole area (○) gives the ratio of the ground state to the first excited state at the burning photon energy. Here, we evaluated the hole area including acoustic phonon wings. Solid and open circles in Fig. 4(a) show the contributions of the ground state and the first excited state of excitons confined in CuCl quantum dots to the absorption spectrum, respectively. To derive Fig. 4(a), we adopted following two assumptions. One is that actual quantum dots are deviated from cubes but preserve their high symmetry. Under this assumption, the ground state E_1 and the first excited state E_2 satisfy the equation $E_2 - E_B \approx 2(E_1 - E_B)$. In fact, our simulated results showed that the three-directional side lengths of quantum boxes should not be different by twice $a/2$ from each other for reproduction of the oscillatory fine structures in the Z_3 exciton absorption band.²¹ Another as-

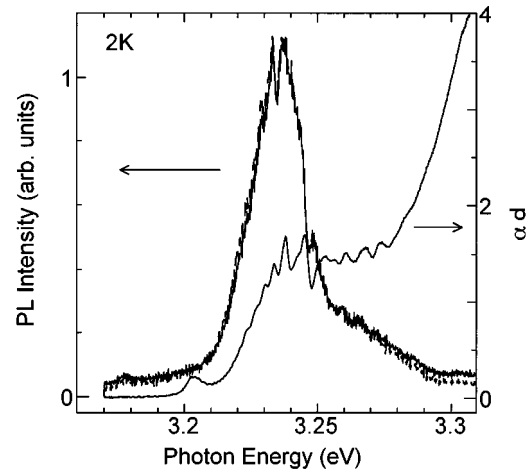


FIG. 5. An absorption and a photoluminescence spectra of CuCl quantum dots in NaCl at 2 K. Excitation photon energy is 3.49 eV for the luminescence spectrum. A dashed line indicates the luminescence spectrum made by the reabsorption correction.

sumption is that only both the first excited state and the ground state contribute to the Z_3 exciton absorption band.

From the obtained spectral profiles in Fig. 4(a), we can estimate the oscillator strength of the ground state (f_1) and the first excited state (f_2). The oscillator strength of the first excited state is equal to zero if quantum dots are cubes. Simultaneously we can compare the obtained ratio f_2/f_1 with that expected for a quantum sphere.²² Theoretical f_2/f_1 for a quantum sphere with radius R is 0.51 for $R/a_B = 5.8$ and 0.59 for $R/a_B = 4.4$, while from Fig. 4(b), the corresponding experimental f_2/f_1 is 0.28 and 0.23, respectively. The experimental oscillator strength ratio f_2/f_1 is about half the ratio for the quantum sphere and does not contradict with our model that the shape of CuCl quantum dots ranges from cubic to spherical while maintaining high symmetry. However, there are few studies concerning the problem how the oscillator strength depends on the shape of quantum dots. Further study is necessary to clarify this difficult problem.

In Fig. 5, absorption and photoluminescence spectra of CuCl quantum dots in NaCl are shown. The luminescence signal was accumulated while the sample was excited by 1800 shots of laser pulses with the very weak energy density of 3.1 $\mu\text{J}/\text{cm}^2$ and the band-to-band excitation photon energy of 3.49 eV. The luminescence spectrum has the same oscillatory structure as the absorption spectrum and shows small Stokes shift (~ 0.6 meV), which suggests that the luminescence spectrum comes from recombination of free excitons confined in CuCl quantum dots. The luminescence spectrum drawn by a dashed line is corrected by taking account of the reabsorption effect and is normalized at the peak energy. We note that the luminescence signal is smaller above 3.25 eV, though the exciton absorption intensity does not decrease so much in this energy region. This fact does not contradict with our idea that the excited states are in the majority at the higher-energy region of the Z_3 exciton absorption band.

In summary, we have observed the excited-state excitons in CuCl quantum cubes by means of the PSHB spectroscopy. Energy positions of satellite holes in the PSHB spectrum show that the shape of quantum dots in NaCl matrix is not

spherical but rather cubic. However, actual quantum dots are considered to be deviated from ideal cubes and have almost continuously distributed shapes without breaking high symmetry. We have determined the spectral profiles of the ground state and the first excited state in CuCl quantum dots. The Z_3 exciton luminescence spectrum showed that the ex-

cited state excitons are in majority at the higher-energy region of the Z_3 exciton absorption band.

We are indebted to Dr. T. Kawazoe and Dr. T. Okuno for their valuable experimental advice and to Dr. S. Nair and Dr. N. Matsuura for valuable discussions.

*Present address: Atsugi Base, Ayase, Kanagawa 252, Japan.

†Author to whom correspondence should be addressed.

¹D. Leonard, M. Krishnamurthy, C. M. Reeves, S. P. Denbaars, and P. M. Petroff, *Appl. Phys. Lett.* **63**, 3203 (1993).

²J. Oshinowo, M. Nishioka, S. Ishida, and Y. Arakawa, *Jpn. J. Appl. Phys. Part 2*, **33**, L1634 (1994).

³C. B. Murray, D. J. Norris, and M. G. Bawendi, *J. Am. Chem. Soc.* **115**, 8706 (1993).

⁴T. D. Bestwick, M. D. Dawson, A. H. Kean, and G. Duggan, *Appl. Phys. Lett.* **66**, 1382 (1995).

⁵F. Heinrichsdorff, A. Krost, M. Grundmann, D. Bimberg, A. Kosogov, and P. Werner, *Appl. Phys. Lett.* **68**, 3284 (1996).

⁶M. Kitamura, M. Nishioka, J. Oshinowo, and Y. Arakawa, *Appl. Phys. Lett.* **66**, 3663 (1995).

⁷D. Fröhlich, M. Haselhoff, K. Reimann, and T. Itoh, *Solid State Commun.* **94**, 189 (1995).

⁸K. Naoe, L. G. Zimin, and Y. Masumoto, *Phys. Rev. B* **50**, 18 200 (1994).

⁹Y. Masumoto, S. Okamoto, T. Yamamoto, and T. Kawazoe, *Phys. Status Solidi B* **188**, 209 (1995).

¹⁰Y. Masumoto, T. Kawazoe, and T. Yamamoto, *Phys. Rev. B* **52**, 4688 (1995).

¹¹Y. Masumoto, K. Kawabata, and T. Kawazoe, *Phys. Rev. B* **52**,

7834 (1995).

¹²J. Qi and Y. Masumoto, *Solid State Commun.* **99**, 467 (1996).

¹³Y. Masumoto, K. Sonobe, and N. Sakakura, *Proceedings of the 23rd International Conference on the Physics of Semiconductors*, edited by M. Scheffler and R. Zimmermann, (Springer-Verlag, Berlin, 1996), p. 1481.

¹⁴A. I. Ekimov, Al. L. Efros, and A. A. Onushchenko, *Solid State Commun.* **56**, 921 (1985).

¹⁵T. Itoh, Y. Iwabuchi, and M. Kataoka, *Phys. Status Solidi B* **145**, 567 (1988).

¹⁶M. Ueta, M. Ikezawa, and S. Nagasaka, *J. Phys. Soc. Jpn.* **20**, 1724 (1965).

¹⁷T. Itoh, S. Yano, N. Katagiri, Y. Iwabuchi, C. Gourdon, and A. I. Ekimov, *J. Lumin.* **60&61**, 396 (1994).

¹⁸Z. K. Tang, A. Yanase, T. Yasui, Y. Segawa, and K. Cho, *Phys. Rev. Lett.* **71**, 1431 (1993).

¹⁹Z. K. Tang, A. Yanase, Y. Segawa, N. Matsuura, and K. Cho, *Phys. Rev. B* **52**, 2640 (1995).

²⁰A. Sacra, D. J. Norris, C. B. Murray, and M. G. Bawendi, *J. Chem. Phys.* **103**, 5236 (1995).

²¹N. Sakakura and Y. Masumoto, *Jpn. J. Appl. Phys.* (to be published).

²²Y. Kayanuma, *Phys. Rev. B* **38**, 9797 (1988).